Fifty-third Annual Allerton Conference
Allerton House, UIUC, Illinois, USA
September 29 - October 2, 2015

Pseudo-gradient Based Local Voltage Control in Distribution Networks

Xinyang Zhou[†], Masoud Farivar[*] and Lijun Chen[†]
[†]College of Engineering and Applied Science, University of Colorado, Boulder
emails: {xinyang.zhou, lijun.chen}@colorado.edu
[*]Department of Electrical Engineering, Caltech, Pasadena
email: mfarivar@caltech.edu

***Abstract*—Voltage regulation is critical for distribution systems, and has become a much more challenging problem with the increasing proliferation of distributed renewable energy resources that cause frequent and rapid voltage fluctuations beyond what can be handled by the traditional voltage regulation methods. In this paper, motivated by the shortcomings of two previously proposed inverter-based local volt/var control algorithms, we design a pseudo-gradient based voltage control algorithm for the distribution network that does not constrain the allowable control functions while admits low implementation complexity. We characterize the convergence of the pseudo-gradient based control scheme, and compare it against the two previous algorithms in terms of the convergence condition and the convergence rate.**

I. NOTATION

$\mathcal{N}$	set of buses excluding bus 0, $\mathcal{N} := \{1, ..., n\}$
$\mathcal{L}$	set of power lines
$\mathcal{L}_i$	set of the lines form bus 0 to bus i
p_i^c, q_i^c	real, reactive power consumption at bus i
p_i^g, q_i^g	real, reactive power generation at bus i
P_{ij}, Q_{ij}	real and reactive power flow from i to j
r_{ij}, x_{ij}	resistance and reactance of line (i, j)
v_i	magnitude of complex voltage at bus i
ℓ_{ij}	squared magnitude of complex current of line (i, j)
x^+	positive part, $x^+ = \max\{0, x\}$
$[x]_{\Omega_i}$	projection of x onto the set Ω_i
$\lambda_{max}(X)$	the maximum eigenvalue of X

A quantity without subscript is usually a vector with appropriate components defined earlier, e.g., $v := (v_i, i \in \mathcal{N}), q^g := (q_i^g, i \in \mathcal{N})$.

II. INTRODUCTION

Both developed and developing countries [5] have been deploying a large amount of distributed renewable generations like photovoltaic (PV) and wind, to keep up with their ever-growing power demand and to ease environmental problems as well. However, renewable generations bring about frequent and rapid voltage fluctuations (at the timescale of seconds) in the distribution system, considerably beyond the reach of traditional voltage regulation methods with capacitor banks and under load tap changers that operate at the timescale of hours. The new IEEE Standard 1547.8 proposes inverter-based volt/var control in the distribution system [3], [4]. Indeed, inverters can push/pull reactive power much faster and in a fine granularity, and can be operated fast enough to keep up with the rapid voltage fluctuation and compensate it. Extensive study has been done to justify the inverter-based volt/var control in the distribution system; see, e.g., [6] - [11].

In particular, motivated by the 1547.8 Standard, the reference [1] has studied a non-incremental inverter-based local volt/var control scheme that decides the reactive power injection at a bus based only on the voltage deviation from the nominal value at the bus, and shown that the non-incremental control can be seen as a distributed algorithm for solving a well-defined convex optimization problem under proper conditions. However, the non-incremental control algorithm has a restrictive convergence condition that constrains the allowable control functions. This has motivated us to propose an incremental voltage control algorithm based on the (sub)gradient algorithm for solving the same optimization problem [2]. Even though the (sub)gradient based voltage control has less restrictive convergence condition, it has a high implementation complexity because of the need to choose the proper subgradient direction and to compute the inverse of the control function. Therefore, in this paper we propose a pseudo-gradient based voltage control algorithm that not only admits a less restrictive convergence condition but also has a low implementation complexity. We show that the dynamical system with the new voltage control algorithm solves the same optimization problem and gives the condition on the stepsize under which the system converges. We further compare all the three voltage control algorithms analytically, as well as numerically based on a real world distribution circuit.

The rest of this paper is organized as follows. Section III presents the system model, and briefly summarizes major results of the non-incremental and (sub)gradient based voltage control algorithms in [1] and [2]. Section IV presents the pseudo-gradient based voltage control algorithm and its convergence analysis. Comparison among all the three voltage control algorithms is presented in Section V, and Section VI concludes the paper.

978-1-5090-1824-6/15/$31.00 ©2015 IEEE

III. System Model

A. Power flow model

We adopt the following branch flow model [13], [15] for a radial distribution system:

$$P_{ij} = p_j^c - p_j^g + \sum_{k:(j,k)\in\mathcal{L}} P_{jk} + r_{ij}\ell_{ij}, \quad (1a)$$

$$Q_{ij} = q_j^c - q_j^g + \sum_{k:(j,k)\in\mathcal{L}} Q_{jk} + x_{ij}\ell_{ij}, \quad (1b)$$

$$v_j^2 = v_i^2 - 2\left(r_{ij}P_{ij} + x_{ij}Q_{ij}\right) + \left(r_{ij}^2 + x_{ij}^2\right)\ell_{ij}, \quad (1c)$$

$$\ell_{ij}v_i = P_{ij}^2 + Q_{ij}^2. \quad (1d)$$

Following [14], [1], we use a linearized version of the above model by letting $\ell_{ij} = 0$ for all $(i,j) \in \mathcal{L}$ in (1). This approximation neglects the higher order real and reactive power loss terms. Since losses are typically much smaller than power flows P_{ij} and Q_{ij}, this only introduces a small relative error, typically on the order of 1% [13]. We further assume that $v_i \approx 1$ so that we can set $v_j^2 - v_i^2 = 2(v_j - v_i)$ in equation (1c).[1] This approximation introduces a small relative error of at most 0.25% (1%) if there is a 5% (10%) deviation in voltage magnitude [1]. With the above approximations, the power flow model (1) simplifies to the following linear model:

$$v = \overline{v}_0 + R(p^g - p^c) + X(q^g - q^c),$$

where $\overline{v}_0 = (v_0, \ldots, v_0)$ is an n-dimensional vector, and resistance matrix $R = [R_{ij}]_{n\times n}$ and reactance matrix $X = [X_{ij}]_{n\times n}$ are symmetric matrices with entries

$$R_{ij} := \sum_{(h,k)\in\mathcal{L}_i\cap\mathcal{L}_j} r_{hk}, \qquad X_{ij} := \sum_{(h,k)\in\mathcal{L}_i\cap\mathcal{L}_j} x_{hk}. \quad (2)$$

In this paper we assume that $\overline{v}_0, p^c, p^g, q^c$ are given constants. The only variables are (column) vectors $v := (v_1, \ldots, v_n)$ of squared voltage magnitudes and $q^g := (q_1^g, \ldots, q_n^g)$ of reactive powers. Let $\tilde{v} = \overline{v}_0 + R(p^g - p^c) - Xq^c$, which is a constant vector. For notational simplicity in the rest of the paper we will ignore the superscript in q^g and write q instead. Then the linearized branch flow model reduces to the following simple form:

$$v = Xq + \tilde{v}. \quad (3)$$

It has been shown in [1] that the matrix X is positive definite.

B. Local volt/var control

The goal of volt/var control on a distribution network is to provision reactive power injections $q := (q_1, \ldots, q_n)$ in order to maintain bus voltages $v := (v_1, \ldots, v_n)$ within a tight range around their nominal values v_i^{nom}, $i \in \mathcal{N}$. This can be modeled by a feedback dynamical system with state $(v(t), q(t))$ at discrete time t. A general volt/var control algorithm maps the current state $(v(t), q(t))$ to a new reactive power injections $q(t+1)$. The new $q(t+1)$ produces a new voltage magnitudes $v(t+1)$ according to (3). Usually $q(t+1)$ is dertermined either completely or partly according to a certain volt/var control function defined as follows:

Definition 1. *A volt/var control function $f : \mathbb{R}^n \to \mathbb{R}^n$ is a collection of $f_i : \mathbb{R} \to \mathbb{R}$ functions, each of which maps the current local voltage v_i to a local control variable o_i in reactive power at bus i:*

$$o_i = f_i(v_i), \quad \forall i \in \mathcal{N}. \quad (4)$$

The control functions f_i are usually decreasing but not always strictly decreasing because of the deadband in control, as well as the bounds of feasible reactive power injections. We assume for each bus $i \in \mathcal{N}$ a symmetric deadband around the nominal voltage $(v_i^{nom} - \delta_i/2, v_i^{nom} + \delta_i/2)$ with $\delta_i \geq 0$. We make the following two assumptions [1]:

- A1: The volt/var control functions f_i are non-increasing over $\mathcal{R}$ and strictly decreasing and differentiable in $(-\infty, v_i^{nom} - \delta_i/2)$ and in $(v_i^{nom} + \delta_i/2, \infty)$.
- A2: The derivative of the control function f_i is bounded, i.e., there exists a finite α_i such that $|f_i'(v_i)| \leq \alpha_i$ for all v_i in the appropriate domain.

As an illustrative example, see Fig. 1 (left) for the piecewise linear droop control function proposed in the latest draft of IEEE 1547.8 Standard [3]:[2]

$$f_i(v_i) := \left[-\alpha_i\left(v_i - v_i^{\text{nom}} - \frac{\delta_i}{2}\right)^+ + \alpha_i\left(-v_i + v_i^{\text{nom}} - \frac{\delta_i}{2}\right)^+\right]_{q_i^{\min}}^{q_i^{\max}}, \quad (5)$$

where the local control variable in reactive power is constrained to within $[q_i^{\min}, q_i^{\max}]$. This particular control function will be used in the numerical examples presented in Section V-B.

1) Non-incremental control algorithm: Motivated by IEEE Standard 1547 [3] [4], we have studied in [1] a local volt/var control where each bus i makes an individual decision $q_i(t+1)$ based only on its own voltage $v_i(t)$, i.e., $q_i(t+1) = o_i(t)$, which we call *non-incremental control* as the current decision on reactive power injection does not depend directly on its previous decision. We thus obtain the following dynamical system that models the non-incremental local volt/var control in the distribution network:

$$D1: \begin{cases} v(t) = Xq(t) + \tilde{v} \\ q(t+1) = f(v(t)). \end{cases} \quad (6)$$

Definition 2. *(v^*, q^*) is called an equilibrium point for $D1$, if*

$$v^* = Xq^* + \tilde{v},$$
$$q^* = f(v^*).$$

By reverse engineering, we have shown in [1] that the dynamical system $D1$ can be seen as a distributed optimization algorithm for solving a well-defined optimization problem

$$\min_{q\in\Omega} \quad F(q) := C(q) + \frac{1}{2}q^T Xq + q^T\tilde{v}, \quad (7)$$

[1] Note that this assumption is not essential and we can also work with v_i^2 instead.

[2] Here we also use α_i to indicate the slope of the droop control function, which does not contradict the use of α_i in the condition A2.

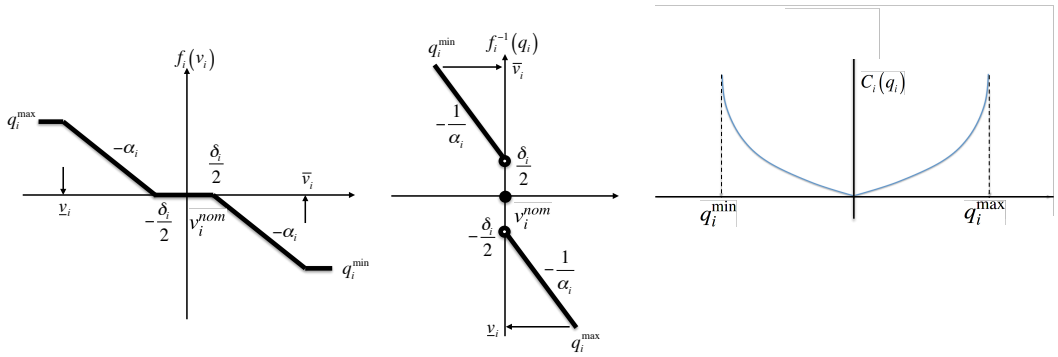

Fig. 1: From left to right: piecewise linear volt/var control curve f_i discussed in the draft of the IEEE 1547 standard [3], its inverse f_i^{-1}, and the corresponding reverse-engineered cost function C_i.

where $C(q) = \sum_{i\in\mathcal{N}} C_i(q_i)$ with a convex cost function for each bus $i \in \mathcal{N}$ defined by $C_i(q_i) := -\int_0^{q_i} f_i^{-1}(q)dq$:

- There exists a unique equilibrium point (v^*, q^*) under condition $A1$; and (v^*, q^*) is an equilibrium point if and only if q^* is the unique optimal solution of (7).
- Under conditions A1-A2, the dynamical system $D1$ converges to the unique equilibrium if the following condition $C1$ holds:

$$C1: \quad A^{-1} > X, \tag{8}$$

where $A^{-1} := \text{diag}(\frac{1}{\alpha_i})$.

As mentioned in [2], the condition $C1$ is hard to verify in practice. First, it is a computationally demanding problem to verify a linear matrix inequality of potentially very large dimensions. Second, matrix X depends on the reactance of every line in the network, which is practically hard to obtain. Moreover, $C1$ is rather restrictive in constraining allowable control functions, and the existing control schemes may not satisfy this condition. We therefore propose in [2] an incremental voltage control based on a (sub)gradient algorithm for solving the optimization problem (7), which leads to a local var/volt control scheme that demands a less restrictive condition for control functions.

2) Incremental control based on (sub)gradient algorithm: By applying (sub)gradient algorithm to the optimization problem (7), we obtain the following dynamical system with an incremental local volt/var control for the distribution network:

$$D2: \left| \begin{array}{lcl} v(t) & = & Xq(t) + \tilde{v} \\ q_i(t+1) & = & \left[q_i(t) - \gamma_g \frac{\partial F(q)}{\partial q_i}\right]_{q_i^{min}}^{q_i^{max}}, \end{array} \right. \tag{9}$$

where $\gamma_g > 0$ is the stepsize, and the (sub)gradient is calculated by

$$\frac{\partial F(q)}{\partial q_i} = \begin{cases} C_i'(q_i(t)) + v_i(t) & \text{if } q_i(t) \neq 0; \\ 0 & \text{if } q_i(t) = 0\ ,\ -\frac{\delta}{2} \le v_i(t) \le \frac{\delta}{2}; \\ -\frac{\delta}{2} + v_i(t) & \text{if } q_i(t) = 0\ ,\ v_i(t) > \frac{\delta}{2}; \\ \frac{\delta}{2} + v_i(t) & \text{if } q_i(t) = 0\ ,\ v_i(t) < -\frac{\delta}{2}. \end{cases} \tag{10}$$

We have the following result [2]:

- Under condition $A1$, the dynamical systems $D1$ and $D2$ have the same, unique equilibrium point (v^*, q^*); and (v^*, q^*) is an equilibrium point if and only if q^* is the unique optimal solution of (7).
- Under condition A1, the dynamical system $D2$ converges to the unique equilibrium if the following condition $C2$ holds:

$$C2: \quad \gamma_g < \frac{2}{\lambda_{max}(\nabla^2 C(q) + X)}, \tag{11}$$

where λ_{max} denotes the maximum eigenvalue.

Compared with $C1$, $C2$ is a much less restrictive: no matter what the reactance matrix X is and no matter what the control functions f_i's are (as long as they satisfy condition A1), we can always find a small enough stepsize γ_g such that $D2$ converges to its unique equilibrium, which solves optimization problem (7).

C. Motivation for new control algorithm

Despite its less restrictive convergence condition $C2$, the (sub)gradient algorithm incurs lots of implementation complexity. The (sub)gradient (10) requires tracking the value of v_i with respect to $\pm\delta_i/2$, and takes different forms accordingly. Furthermore, it requires the inverse of control functions f_i's, which is computationally expensive for general control functions. This high implementation complexity of gradient algorithm motivates us to seek an incremental voltage control algorithm that not only admits a less restrictive condition on the control function (as the (sub)gradient algorithm does) but also has a low implementation complexity. In next section, we will present such a control algorithm based on pseudo-gradient algorithm for optimization problem (7) and study its equilibrium and dynamical properties.

IV. Pseudo-gradient based local voltage control

Consider the following incremental local voltage control based on the pseudo-gradient algorithm for solving optimiza-

tion problem (7):

$$\begin{aligned} q_i(t+1) &= [(1-\gamma_p)q_i(t) + \gamma_p f_i(v_i(t))]_{q_i^{min}}^{q_i^{max}} \\ &= \Big[q_i(t) - \gamma_p\Big(q_i(t) - f_i(v_i(t))\Big)\Big]_{q_i^{min}}^{q_i^{max}}, \end{aligned} \quad (12)$$

where $\gamma_p > 0$ is the stepsize or the weight. Given control functions f_i's, the implementation of the algorithm (12) is straightforward and does not have any implementation issues that the (sub)gradient based control algorithm in (9) has; see the discussion in Section III-C. It is also interesting to notice that, when the weight $\gamma_p = 1$, we recover the non-incremental voltage control in (6).

With the control (12), we obtain the following dynamical system:

$$D3: \left| \begin{array}{lcl} v(t) & = & Xq(t) + \tilde{v} \\ q_i(t+1) & = & \Big[q_i(t) - \gamma_p\Big(q_i(t) - f_i(v_i(t))\Big)\Big]_{q_i^{min}}^{q_i^{max}}. \end{array} \right. \quad (13)$$

The dynamical system $D3$ has the same equilibrium condition as the dynamical system $D1$. The following result is immediate.

Theorem 1. *Suppose A1 holds. There exists a unique equilibrium point for the dynamical system D3. Moreover, a point (v^*, q^*) is an equilibrium if and only if q^* is the unique optimal solution of problem (7) and $v^* = Xq^* + \tilde{v}$.*

We now analyze the convergence of the dynamical system $D3$.

Lemma 1. *Suppose A1-A2 hold. With any $q_a, q_b \in [q_i^{min}, q_i^{max}]$, we have*

$$\Big((-f_i^{-1}(q_a)) - (-f_i^{-1}(q_b))\Big)(q_a - q_b) \geq \frac{1}{\alpha_i}(q_a - q_b)^2. \quad (14)$$

Proof: By condition $A2$, $|f_i'(v_i)| \leq \alpha_i$. Therefore, the derivative of the inverse of function f_i satisfies $|(f_i^{-1}(q_i))'| = |\frac{1}{f'(f^{-1}(q_i))}| \geq \frac{1}{\alpha_i}$.

If q_a and q_b are both positive (or both negative), then the corresponding $v_a = f_i^{-1}(q_a)$ and $v_b = f_i^{-1}(q_b)$ are both smaller than $v_i^{nom} - \delta_i/2$ (or both larger than $v_i^{nom} + \delta_i/2$). We thus have $|(-f_i^{-1}(q_a)) - (-f_i^{-1}(q_b))| \geq \frac{1}{\alpha_i}|q_a - q_b|$. Equality is achieved if a linear control function, e.g., (5), is used. On the other hand, if one of q_a and q_b is positive and the other is negative, then as long as $\delta \neq 0$, we have $|(-f_i^{-1}(q_a)) - (-f_i^{-1}(q_b))| > \frac{1}{\alpha_i}|q_a - q_b|$. Given the monotonicity of f^{-1}, inequality (14) follows. ∎

Theorem 2. *Suppose A1-A2 hold. If the stepsize γ_p satisfies the following condition C3:*

$$C3: \quad \gamma_p < \frac{2}{\max\{\alpha_i\}\lambda_{max}(\nabla^2 C(q) + X)}, \quad (15)$$

then the dynamical system D3 converges to its unique equilibrium.

Proof: Consider first the case when $q_i(t) \neq 0$, $\forall i$, i.e., when objective function F is differentiable. By the second-order Taylor expansion, we have

$$\begin{aligned} & F(q(t+1)) \\ = \; & F(q(t)) - \gamma_p \sum_{i \in \mathcal{N}} (-f_i^{-1}(q_i(t)) + v_i(t))(q_i(t) - f_i(v_i(t))) \\ & + \frac{\gamma_p^2}{2}(q(t) - f(v(t)))^T(\nabla^2 C(\tilde{q}) + X)(q(t) - f(v(t))), \end{aligned} \quad (16)$$

where $f(v(t)) := \Big(f_1(v_1(T)), \ldots, f_n(v_n(t))\Big)^T$, and $\tilde{q} = \theta q(t) + (1-\theta)q(t+1)$ for some $\theta \in [0,1]$. By Lemma 1, we have $(-f_i^{-1}(q_i(t)) + v_i(t))(q_i(t) - f_i(v_i(t))) \geq \frac{1}{\alpha_i}(q_i(t) - f_i(v_i(t)))^2$. Thus the Taylor expansion follows as

$$\begin{aligned} & F(q(t+1)) \\ \leq \; & F(q(t)) + \frac{1}{2}(q(t) - f(v(t)))^T \\ & (\gamma_p^2(\nabla^2 C(\tilde{q}) + X) - 2\gamma_p A^{-1})(q(t) - f(v(t))). \end{aligned} \quad (17)$$

When condition $C3$ holds, $\gamma_p^2(\nabla^2 C(\tilde{q}) + X) - 2\gamma_p A^{-1}$ is negative definite. So the second term in (17) is non-positive and is equal to zero if and only if $q(t) = f(v(t))$, or equivalently, $q(t) = q(t+1)$. Therefore, $F(q(t+1)) \leq F(q(t))$, and the equality is achieved if and only if $q(t+1) = q(t)$. Moreover, due to the uniqueness of the equilibrium as shown in Theorem 1, $F(q(t+1)) = F(q(t))$ if and only if $q(t+1) = q(t) = q^*$. So, F is a discrete-time Lyapunov function for the dynamical system $D3$, and by the Lyapunov stability theorem, the equilibrium q^* is globally asymptotically stable [16].

Consider next the case when $q_i(t) = 0$ for some i, at which $C_i(q_i(t))$ is non-smooth. Therefore, we need to carefully define the derivative used in the Taylor expansion. For the first order derivatives, we can choose

$$\frac{\partial F(q)}{\partial q_i} = \left\{ \begin{array}{ll} C_i'(q_i(t)) + v_i(t) & \text{if } q_i(t) \neq 0 \\ 0 & \text{if } \; q_i(t) = 0 \; , \; -\frac{\delta}{2} \leq v_i(t) \leq \frac{\delta}{2} \\ -\frac{\delta}{2} + v_i(t) & \text{if } \; q_i(t) = 0 \; , \; v_i(t) > \frac{\delta}{2} \\ \frac{\delta}{2} + v_i(t) & \text{if } \; q_i(t) = 0 \; , \; v_i(t) < -\frac{\delta}{2} \end{array} \right. .$$

The second order derivatives can be defined as the right or left derivative of the above chosen first order derivatives. With these well-defined derivatives, the proof follows similarly as the case with $q_i(t) \neq 0$, $\forall i$.

∎

Theorem 2 shows that, like the (sub)gradient based voltage control, the pseudo-gradient based control has a convergence condition that does not constrain the allowable control functions f_i. We will provide more detailed comparison between the above three local voltage control algorithms in the next section.

Remarks: Notice that in the pseudo-gradient algorithm it is usually assumed that $\gamma_p \leq 1$. This gives a nice interpretation of the new decision $q_i(t+1)$ being a (positively-)weighted sum of the decision $q_i(t)$ at the previous time and the local control $o_i(t) = f_i(v(t))$ in reactive power. However, here we do not require $\gamma_p \leq 1$, as long as condition $C3$ is satisfied.

V. Comparative Study of Convergence Conditions and Rates

We have presented three different local voltage control algorithms in the previous two sections. In this section, we compare these three control schemes in terms of the convergence condition and the convergence rate. As will be seen, the (sub)gradient and pseudo-gradient based algorithms have very close performance. Therefore, as discussed in the previous sections, the advantage of the pseudo-gradient based algorithm over the gradient based algorithm is its lower implementation complexity. This low implementation complexity, however, provides strong enough motivation for adopting the pseudo-gradient based local voltage control in the distribution network.

A. Analytical characterization

1) Comparison between D3 and D1: As mentioned earlier, $D1$ can be seen as a special case of $D3$.

Proposition 1. *The non-incremental voltage control in the dynamical system $D1$ is a special case of the control in $D3$ with the stepsize $\gamma_p = 1$.*

As a result of Proposition 1, when condition $C1$ holds, the largest stepsize that $D3$ can take is no smaller than 1. On the other hand, if condition $C3$ gives an upper bound for γ_p that is smaller than 1, $D1$ will not converge.

2) Comparison between D3 and D2: We investigate the relationship between the dynamical systems $D2$ and $D3$, in terms of the available ranges of the stepsizes γ_g and γ_p for convergence, as well as the convergence rates by looking at descent rates of their objective values. We will see that $D2$ and $D3$ are closely related, and even equivalent under certain circumstances.

Proposition 2. *There is a one-to-one correspondence between the ranges of the convergence stepsizes γ_g and γ_p of the dynamical systems $D2$ and $D3$, i.e., for any $\gamma_p \in (0, B_p]$, there is a corresponding $\gamma_g = \max\{a_i\}\gamma_p \in (0, B_g]$, where B_g and B_p are the upper bounds on the stepsize given in conditions $C2$ and $C3$ respectively.*

Proof: The result follows from the proofs of the sufficiency of the conditions $C2$ and $C3$ for convergence. ■

Moreover, we expect similar convergence rates, or descent rates for the dynamical systems $D2$ and $D3$.

Proposition 3. *The dynamical systems $D2$ and $D3$ have convergence rates of the same order when the corresponding stepsizes are chosen.*

Proof: Pick a convergence stepsize γ_p for $D3$ and a corresponding convergence stepsize $\gamma_g = \max\{a_i\}\gamma_p$ for $D2$. By the second-order Taylor expansion, the descent in the objective value $F(q(t+1)) - F(q(t))$ of the pseudo-gradient algorithm is roughly given as

$$\frac{1}{2}\Big(q(t) - f(v(t))\Big)^T\Big(\gamma_p^2(\nabla C(\tilde{q}) + X) - 2\gamma_p A^{-1}\Big)\Big(q(t) - f(v(t))\Big), \quad (18)$$

while that of the gradient algorithm is given as

$$\frac{1}{2}\Big(v(t) - f^{-1}(q(t))\Big)^T\Big(\gamma_g^2(\nabla C(\tilde{q}) + X) - 2\gamma_g I\Big)\Big(v(t) - f^{-1}(q(t))\Big). \quad (19)$$

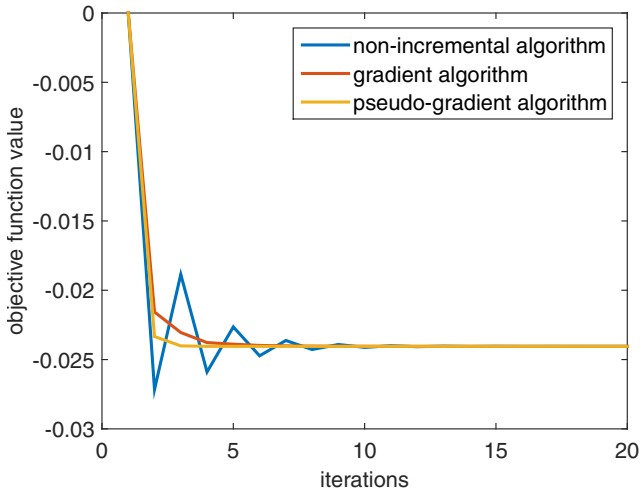

Fig. 3: $D1$, $D2$ and $D3$ all converge

Notice that from the proof of Lemma 1, there exists a factor of $\max\{\alpha_i\}$ between $(q(t) - f(v(t)))$ and $(v(t) - f^{-1}(q(t)))$, which compensates the factor $1/\max\{a_i\}$ between γ_p and γ_g. As a result, the above two decent terms are in the same order, with the only difference coming from the gap between A and $\max\{\alpha_i\}I$. ■

Consider a system where all the buses have identical control functions f_i. Since $A = \max\{\alpha_i\}I$, the following result is immediate.

Corollary 1. *The dynamical systems $D2$ and $D3$ have the same convergence rates if an identical control functions are used at all buses.*

B. Numerical examples

We now provide numerical examples to complement the theoretical analysis in the previous (sub)sections, based on the piecewise linear droop control functions (5). The network topology (Fig. 2) and parameters (TABLE I) are based on a distribution feeder of South California Edison. As shown in Fig. 2, the bus 1 is the actual the "0" bus, and five PVs are installed on buses 2, 12, 26, 29, and 31 respectively.[3] AC power flow model is applied in our simulations, calculated with MatLab package MatPower [17], instead of the linear model we use in the analytical characterization.

The deadband for control is chosen to be $[0.98^{p.u.}, 1.02^{p.u.}]$ for all the buses, and the hard voltage thresholds $\overline{v}_i$ and $\underline{v}_i$ in control functions are designed to be variables, adjusted for the purpose of comparison of convergence conditions with $\alpha_i = q_i^{max}/(\overline{v}_i - \delta/2)$.

[3]Different from what is implied in the system model and its analysis, in practice we may not have control at all the buses. As a result, the convergence analysis needs to be modified accordingly, based on an "effective" reactance matrix that takes into consideration the buses without control.

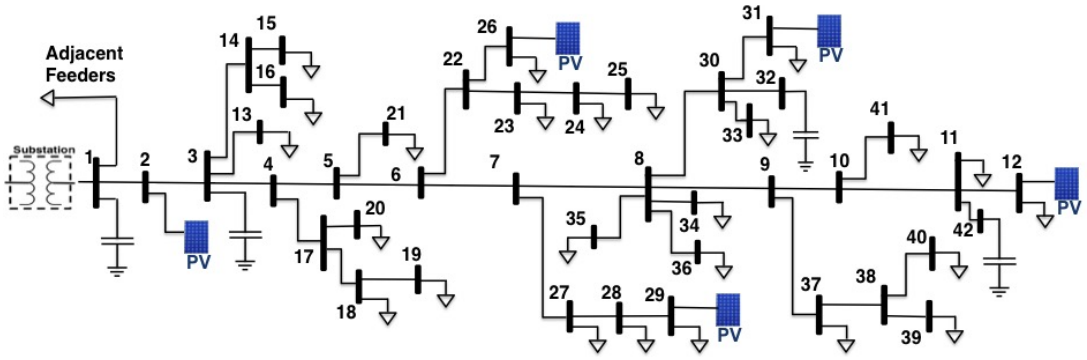

Fig. 2: Circuit diagram for SCE distribution system.

TABLE I: Network of Fig. 2: Line impedances, peak spot load KVA, Capacitors and PV generation's nameplate ratings.

Network Data																	
Line Data				Line Data				Line Data				Load Data		Load Data		PV Generators	
From Bus.	To Bus.	R (Ω)	X (Ω)	From Bus.	To Bus.	R (Ω)	X (Ω)	From Bus.	To Bus.	R (Ω)	X (Ω)	Bus No.	Peak MVA	Bus No.	Peak MVA	Bus No.	Capacity MW
1	2	0.259	0.808	8	34	0.244	0.046	18	19	0.198	0.046	11	0.67	28	0.27		
2	3	0.031	0.092	8	36	0.107	0.031	22	26	0.046	0.015	12	0.45	29	0.2	2	1
3	4	0.046	0.092	8	30	0.076	0.015	22	23	0.107	0.031	13	0.89	31	0.27	26	2
3	13	0.092	0.031	8	9	0.031	0.031	23	24	0.107	0.031	15	0.07	33	0.45	29	1.8
3	14	0.214	0.046	9	10	0.015	0.015	24	25	0.061	0.015	16	0.67	34	1.34	31	2.5
4	17	0.336	0.061	9	37	0.153	0.046	27	28	0.046	0.015	18	0.45	35	0.13	12	3
4	5	0.107	0.183	10	11	0.107	0.076	28	29	0.031	0	19	1.23	36	0.67		
5	21	0.061	0.015	10	41	0.229	0.122	30	31	0.076	0.015	20	0.45	37	0.13		
5	6	0.015	0.031	11	42	0.031	0.015	30	32	0.076	0.046	21	0.2	39	0.45		
6	22	0.168	0.061	11	12	0.076	0.046	38	39	0.107	0.015	23	0.13	40	0.2		
6	7	0.031	0.046	14	16	0.046	0.015	38	40	0.061	0.015	24	0.13	41	0.45		
7	27	0.076	0.015	14	15	0.107	0.015	43	44	0.061	0.015	25	0.2	V_{base} = 12.35 KV			
7	8	0.015	0.015	17	18	0.122	0.092	43	45	0.061	0.015	26	0.07	S_{base} = 1000 KVA			
8	35	0.046	0.015	17	20	0.214	0.046					27	0.13	Z_{base} = 152.52 Ω			

1) Convergence condition: We start with observing the difference in the convergence conditions between the three control algorithms.

- We first show in Fig.3 that, once we design the control functions and choose the stepsizes such that the convergence conditions $C1 - C3$ are met, the dynamical systems $D2$ and $D3$ converge monotonically to the same equilibrium. However, the dynamical system $D1$ converges but may not converge monotonically.
- We then change the slopes of the control functions such that we have a larger A^{-1} (i.e., smaller α_i). This will give $D2$ a more strict condition and $D3$ a less strict one. Resultantly, as shown in Fig.4(a), $D2$ no longer converges. However, by decreasing the stepsize γ_g, $D2$ can be brought back to convergence, as shown in Fig. 4(b).
- Lastly, we change the slopes of control functions to get a smaller A^{-1} (i.e., larger α_i). This affects the convergence conditions for $D1$ and $D3$, while leaving that for $D2$ in-violated. Similarly, $D3$ can be brought back to convergence by choosing a smaller stepsize. This is shown in Fig. 4(c)-(d).

2) Range of the stepsize for convergence: Proposition 2 shows that the upper bounds for the convergence stepsizes of $D2$ and $D3$ are related by a factor of $\max\{\alpha_i\}$, and it is interesting to see how tight this factor is. For the linear control function, $\max\{\alpha_i\} = \max(q_i^{max}/(\overline{v} - \delta/2))$, assuming the same and symmetric hard voltage threshold $\overline{v} - v^{nom} = v^{nom} - \underline{v}$ at all buses. We tune $\overline{v}$ such that the value of $\overline{v} - v^{nom}$ ranges from $0.03^{p.u.}$ to $0.18^{p.u.}$ with granularity of $0.01^{p.u.}$, and the value of $\max(\alpha_i)$ ranges from 158 to 9.84 accordingly. We examine the largest possible stepsize $\max(\gamma_g)$ and $\max(\gamma_p)$, and compare their ratio with the factor $\max(\alpha_i)$. The granularity for γ_g and γ_p is 1 and 0.05 respectively. Fig.5 shows that the ratio between the convergence ranges for the gradient algorithm and pseudo-gradient algorithm is close to $\max\{\alpha_i\}$. This confirms Proposition 2.

3) Convergence rate: We study the convergence rates under certain fixed control functions, with stepsizes γ_g and γ_p varied within the convergence ranges.[4] Notice that $D1$ is a special case of $D3$ with $\gamma_p = 1$.

We choose the hard voltage threshold as $\underline{v}_i = 0.92^{p.u.}$ and $\overline{v}_i = 1.08^{p.u.}$, and vary the stepsize until it reaches the convergence condition boundary. As shown in Fig. 6 and

[4]Since the simulations are run under the nonlinear model, the boundary for convergence stepsizes will usually be different from that obtained under the linear model. We carefully choose the values of the stepsize so that the convergence results can still be obtained.

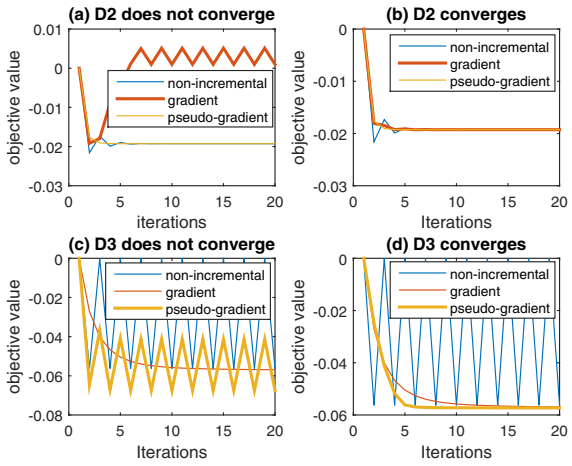

Fig. 4: D2 and D3 can be brought back to convergence by choosing small enough stepsizes γ_g and γ_p.

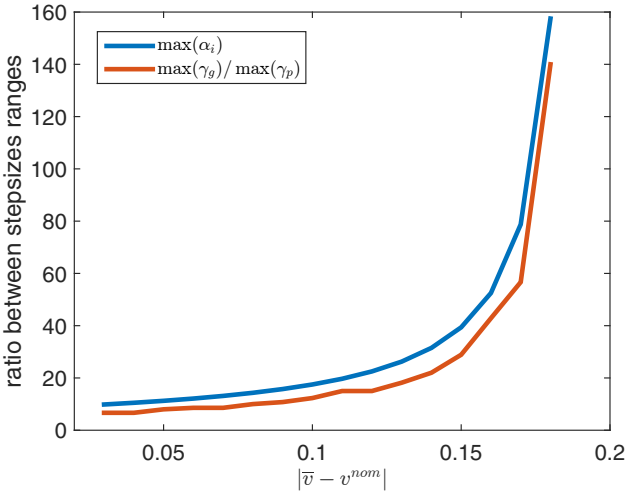

Fig. 5: The upper bounds for γ_g and γ_p are related by a factor close to $\max(\alpha_i)$.

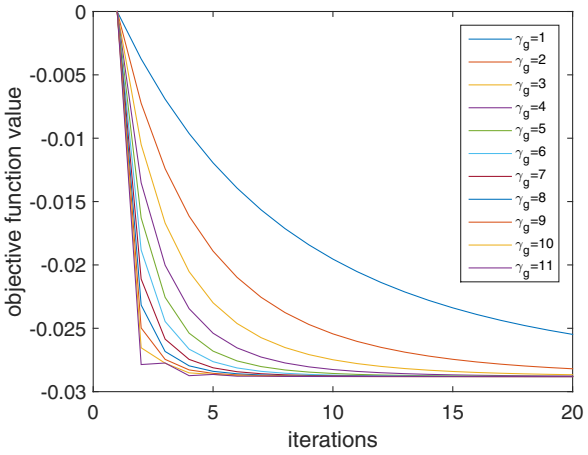

Fig. 6: Convergence rate of the gradient algorithm with different stepsizes: larger γ_g leads to faster convergence.

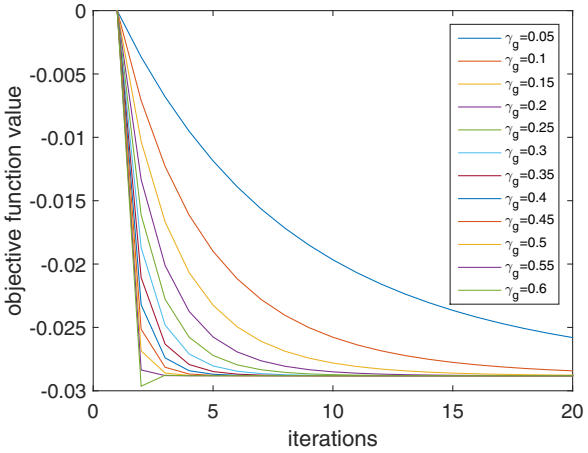

Fig. 7: Convergence rate of the pseudo-gradient algorithm with different stepsizes: larger γ_p leads to faster convergence.

Fig. 7, the convergence rates for both gradient algorithm and pseudo-gradient algorithm increase monotonically with the stepsizes before they reach the upper bounds. Also, both algorithms perform similarly in terms of the convergence rate.

VI. Conclusion

Motivated by the shortcomings of two previously proposed inverter-based local volt/var control algorithms, we have proposed a pseudo-gradient based voltage control algorithm for the distribution network that does not constrain the allowable control functions while admits low implementation complexity. We characterize the convergence of the pseudo-gradient based control scheme, and compare it against the two previous algorithms in terms of the convergence condition and the convergence rate as well.

References

[1] M. Farivar, L. Chen, and S. Low, "Equilibrium and dynamics of local voltage control in distribution systems," 52nd IEEE Annual Conference on Decision and Control (CDC), pp. 4329–4334, 2013.

[2] M. Farivar, X. Zhou, and L. Chen, "Local Voltage Control in Distribution System: An Incremental Control Algorithm," submitted for publication, 2015.

[3] Standards Coordinating Committee 21 of Institute of Electrical and Electronics Engineers, Inc., IEEE Standard P1547.8™/D8, "Recommended Practice for Establishing Methods and Procedures that Provide Supplemental Support for Implementation Strategies for Expanded Use of IEEE Standard 1547", IEEE ballot document, Aug 2014.

[4] Institute of Electrical and Electronics Engineers, Inc., "IEEE Standard 1547a™(2014) Standard for Interconnecting Distributed Resources with Electric Power Systems Amendment 1", May 2014.

[5] J. L. Sawin, F. Sverrisson, "Renewables 2014: Global Status Report", Paris: REN21 Secretariat REN21, 2014.

[6] K. Turitsyn, P. Sulc, S. Backhaus, and M. Chertkov, "Options for control of reactive power by distributed photovoltaic generators, Proceedings of the IEEE, 99(6): 1063-1073, 2011.

[7] J. Smith, W. Sunderman, R. Dugan, and B. Seal, "Smart inverter volt/var control functions for high penetration of pv on distribution systems, *IEEE Power Systems Conference and Exposition (PSCE)*, pp. 1-6, 2011.

[8] M. Farivar, C. R. Clarke, S. H. Low, and K. M. Chandy. "Inverter VAR control for distribution systems with renewables," IEEE SmartGridComm, pp. 457–462, 2011.

[9] B. A. Robbins, C. N. Hadjicostis, and A. D. Dominguez-Garcia, "A two-stage distributed architecture for voltage control in power distribution systems,", IEEE Trans. on Power Systems, 28(2): 1470-1482, 2013.

[10] P. Jahangiri, D. C. Aliprantis, "Distributed Volt/VAr Control by PV Inverters," Power Systems, IEEE Transactions on , vol.28, no.3, pp.3429-3439, 2013

[11] J. Neely, S. Gonzalez, M. Ropp, D. Schutz, "Accelerating Development of Advanced Inverters: Evaluation of Anti-Islanding Schemes with Grid Support Functions and Preliminary Laboratory Demonstration," Sandia National Laboratories Technical Report SAND2013-10231, 2013.

[12] P. Jahangiri, D. C. Aliprantis, "Distributed Volt/VAr Control by PV Inverters," Power Systems, IEEE Transactions on , vol.28, no.3, pp.3429-3439, 2013

[13] M. E. Baran, F. F Wu, "Optimal Capacitor Placement on radial distribution systems", IEEE Trans. Power Delivery, 4(1):725-734, 1989.

[14] M. E. Baran, F.F. Wu, "Network reconfiguration in distribution systems for loss reduction and load balancing", IEEE Transaction on Power Delivery, 4(2): 401-1407, 1989.

[15] M. Farivar and S. H. Low. "Branch flow model: relaxations and convexification (parts I, II)," *Power Systems, IEEE Transactions on*, 28(3):2554-2572, 2013.

[16] H. K. Khalil and J. W. Grizzle, "Nonlinear systems", 3rd Edition, Prentice hall, 200.

[17] Zimmerman, Ray D and Murillo-Sánchez, Carlos E and Gan, Deqiang, "MATPOWER: A MATLAB power system simulation package", Manual, Power Systems Engineering Research Center, Ithaca NY, vol. 1, 1997.